Ученые записки Таврического национального университета имени В.И. Вернадского
Серия «Физико-математические науки». Том 23 (62). 2010 г. № 1. Ч. I. С. 30-56

УДК 535.2:548.1.022/.024

QUADREFRINGENCE OF THE VORTEX BEAMS IN BIREFRINGENT CRYSTALS

Fadeyeva T.A., Rubass A.F., Volyar A.V.

Physics Department, Taurida National V.I. Vernadsky University, Simferopol, Ukraine
E-mail: volyar@crimea.edu

We have found the asymmetric splitting of a high-order circularly polarized vortex-beam in a uniaxial crystal. The l-order vortex-beam splits into the same one and the beam with the l-1 vortices at the beam axis while one optical vortex is shifted along the direction perpendicular to the inclination plane of the beam. Such a vortex displacement causes the transverse shift of the partial beam. We consider this effect both in terms of the conservation law of the angular momentum flux and on the base of the solutions to the paraxial wave equation. We revealed that the transverse shift of the crystal traveling beam depends on neither a magnitude nor a sign of the vortex topological charge being defined only by a handedness of the initial circular polarization and a sign of the inclination angle of the beam.
Keywords: uniaxial crystal, laser radiation, topological charge, optical vortex, polarization status, polarization singularity.

I. INTRODUCTION

The concept of the propagation of a plane wave (or a light ray associated with it) through a homogeneous anisotropic medium (or an unbounded crystal) presented by the Fresnel formulas [1] is a commonplace in physical optics. Transmitting obliquely to the crystal optical axis a light ray splits into two ones – the ordinary and extraordinary rays with orthogonal linear polarizations. However, in most real cases, we deal with a light beam that represents a coherent bundle of rays (plane waves) with different light velocities and directions of the electric and wave vectors. Naturally, the light beam in the crystal can manifest new properties different from those in a separate plane wave. For example, an axially symmetric beam in a uniaxial crystal can be converted into an astigmatic beam [2, 3] whereas the conical refraction of the beams in a biaxial crystal embeds unique singular points (so called the diabolical points) in the beam wavefront [4]. Of even greater dramatic case is the propagation of Gaussian [5-7] and singular beams [8] along the optical axis of a uniaxial crystal. In this connection it should be noted that the singular beam (or the vortex-beam) represents a wave structure containing a set of optical vortices [9] i.e. the phase singularities of the wavefront where the field amplitude is zero while the phase is uncertain. The optical vortex is characterized by a topological charge l equal to a number of wavefront branches in the vicinity of the singular point. The propagation of a singular beam in free space or a homogeneous isotropic medium obeys a simple requirement: a total vortex topological charge does not change when propagating [10]. Specific features have scalar random 3D wave fields where the optical vortices manifest Brownian scaling properties [11]. The most general case represents a vector light field with a spectrum of new unexpected properties of polarization singularities considered in

detail in the seminal work [12] by Nye. Recently Dennis [13] and Flossmann et. al. [14] have theoretically and experimentally supplemented this complex picture with 3D structures of randomly polarized optical fields. Generally speaking, an elliptically polarized vortex-beam carries over a spin and orbital angular momentum [15]. The spin angular momentum (SAM) is associated with a circular polarization of the beam field while the orbital angular momentum (OAM) is characterized by the beam structure, in particular, by the optical vortices imbedded in the beam wavefront. A total angular momentum (i.e. a sum of the OAM and SAM) is conserved for any propagation direction of the beam in free space and homogeneous media. However the above requirements get broken in an anisotropic homogeneous medium [5-8] even for the beam transmitting along a crystal optical axis. At the same time, Ciattoni et. al. [16] have shown that a total angular momentum flux along the crystal optical axis is conserved. The mutual conversion of the SAM and OAM is specified by the spin-orbit coupling [17].

When tilting a singly charged vortex-beam relative to the crystal optical axis, the phase singularities are subjected to a radical reconstruction [18,19] in circularly polarized components relative to those in the beam propagating along the crystal optical axis, the vortex-beam experiencing the asymmetric splitting. We have treated this effect [18] as a result of complex chains of dislocation reactions in each circularly polarized component and termed it the vortex *quadrefringence* i.e. a splitting of the initial singly charged vortex into four identical vortices. Dislocation reactions in the tilted splintered beam entail shifts of the center of gravity of the beam relative to the beam axis. It should be expected that the beam shift vanishes in the asymptotic case when a mutual overlapping of the splintered beams is negligibly small. However, we found [18] that in the asymptotic case, the optical vortices have a residual displacement in the orthogonally circularly polarized component relative to that with the initial circular polarization.

The aim of the given paper is to bring to light the underlining processes that reduce to the asymmetric splitting of the high order tilted vortex-beams and estimate the value of the transverse shift of the beams in one of the circularly polarized components.

II. DESTRUCTION AND RECOVERY OF HIGH ORDER VORTEX-BEAMS

II.1 The basic groups of vortex-beams

We will consider an unbounded homogeneous anisotropic medium with the only optical axis directed along the *z*-axis of the referent frame x,y,z (Fig.1) that characterized by a permittivity tensor in a diagonal form: $diag\ \hat{\varepsilon} = diag\left(\varepsilon_o, \varepsilon_o, \varepsilon_3\right)$, where $n_o = \sqrt{\varepsilon_o}$ and $n_3 = \sqrt{\varepsilon_3}$ being the refractive indices along a major crystallographic axes, $n_o > n_e$ (see Fig.1).We assume at first that the paraxial beam propagates along the crystal optical axis: $\mathbf{E}(x, y, z) = \widetilde{\mathbf{E}}(x, y, z)\exp(-i\, k_o z)$, where $k_o = n_o k_0$ is a wavenumber of the ordinary beam in the crystal, k_0 is a wavenumber in free space.

The paraxial wave equation for the transverse component of the electric vector $\widetilde{\mathbf{E}}_\perp = \mathbf{e}_x \widetilde{E}_x + \mathbf{e}_y \widetilde{E}_y$ ($\mathbf{e}_x, \mathbf{e}_y$ are the unit vectors) can be written in the form [2, 8, 18]:

$$\left(\nabla_\perp^2 - 2ik_o\partial_z\right)\widetilde{\mathbf{E}}_\perp = \beta\nabla_\perp\left(\nabla_\perp\widetilde{\mathbf{E}}_\perp\right), \tag{1}$$

where $\beta = \Delta\varepsilon/\varepsilon_3$, $\Delta\varepsilon = \varepsilon_3 - \varepsilon$. Let us make use of new coordinates: $u = x + iy$, $v = x - iy$ and a new polarization basis: $\widetilde{E}_+ = \widetilde{E}_x - i\widetilde{E}_y$, $\widetilde{E}_- = \widetilde{E}_x + i\widetilde{E}_y$ are the right hand (RHP) and left hand (LHP) circularly polarized components of the beam.

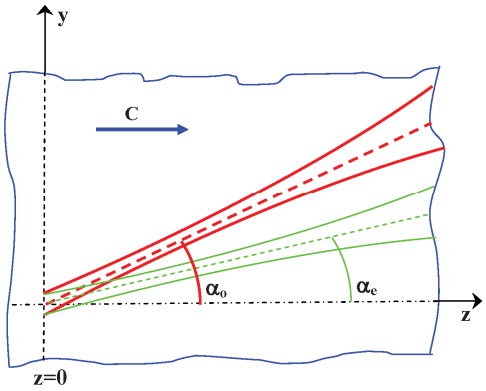

Fig. 1. Sketch of the beam propagation in a uniaxial crystal. **C** is a unit vector of the crystal optical axis.

Then the eq. (5) can be rewritten as

$$\left(4\partial_{uv}^2 - 2ik_o\partial_z\right)\tilde{E}_+ = 2\beta\partial_u\left(\partial_v\tilde{E}_+ + \partial_u\tilde{E}_-\right), \tag{2a}$$

$$\left(4\partial_{uv}^2 - 2ik_o\partial_z\right)E_- = 2\beta\partial_v\left(\partial_vE_+ + \partial_uE_-\right). \tag{2b}$$

Particular solutions to the eqs (2) can be found by means of simple substitutions:

1) the ordinary mode beam:

$$\widetilde{E}_+^o = w_0\,\partial_u\Psi_o, \qquad \tilde{E}_-^o = -w_0\,\partial_v\Psi_o\ , \tag{3}$$

2) the extraordinary mode beam:

$$\widetilde{E}_+^e = w_0\,\partial_u\Psi_e, \qquad \widetilde{E}_-^e = w_0\,\partial_v\Psi_e \tag{4}$$

The scalar function Ψ is a solution to a scalar paraxial wave equation:

$$\left(\nabla_\perp^2 - 2ik_{o,e}\partial_z\right)\Psi_{o,e} = 0 \tag{5}$$

where $k_e = \left(n_3^2/n_o\right)k_0$ being a wavenumber of an extraordinary beam, w_0 is the beam waist at the plane $z = 0$.

A small inclination of the ordinary beam axis relative to the crystal optical axis (say, on the y0z plane) at a small angle $\alpha_o << 1$ can be taken into account by a displacement of the origin of the coordinates along the imaginary *y*-axis at the distance $y_o = i\alpha_o z_o$ [18, 20, 21], where $z_o = k_o w_0^2/2$. The new transverse coordinates are $\bar{x} = x$, $\bar{y} = y + i\alpha_o z_o$, $\bar{u} = u - \alpha_o z_o$, $\bar{v} = v + \alpha_o z_o$. In this case, the paraxial ordinary beam with a Gaussian envelope tilted relative to the z-axis at the angle α_o is transformed into

the beam propagating along the z-axis but its intensity maximum is shifted at the distance $y_o' = y - \alpha_o z$. The extraordinary beam is tilted at the angle α_e and its y-coordinate is shifted at the distance $y_e = i\alpha_e z_e$ ($z_e = k_e w_0^2 / 2$). The transformations of the phase in the tilted extraordinary beam are taken into account by the additional curvatures of the wavefront stimulated by the complex shift $i\alpha_e z_e$. Besides, the function of the Gaussian envelopes get an amplitude factors: $\exp\left(-k_{o,e} z_{o,e} \alpha_{o,e}^2 / 2\right)$. Clearly the solutions (3, 4) to the equations (5) in the coordinates x, y, z also satisfy to these equations in the coordinates $\overline{x}, \overline{y}_{o,e}, z$.

It is worth to note that the operator $\partial_{\overline{u}} = \partial_u = \partial_x - i\partial_y$ acting on the generatrix function of the beam Ψ_0 in free space [22] is the operator of the birth of the vortex-beams with a negative topological charge $l < 0$ while the operator $\partial_{\overline{v}} = \partial_v = \partial_x + i\partial_y$ is the operator of the birth of the positively charged vortex-beams $(l > 0)$. Thus, by acting the operators ∂_u and ∂_v on a generatrix functions $\Psi_0^{(o,e)}$ in the crystal we can create the first large group of the high order vortex-beams. As a generatrix function $\Psi_0^{(o,e)}$ we can choose the functions of the fundamental Gaussian beam in a homogeneous isotropic medium with refractive indices n_o and n_e, respectively:

$$\Psi_0^{(o,e)} = \frac{1}{\sigma_{o,e}} \exp\left[-\frac{\overline{u}\,\overline{v}}{w_0^2 \sigma_{o,e}} - k_{o,e} z_{o,e} \frac{\alpha_{o,e}^2}{2} \right], \tag{6}$$

where $\sigma_{o,e} = 1 - i z / z_{o,e}$. Thus the fields of the high order vortex-beams of the first group V are

$$V_+^{(-l),(o,e)} = N_l^V \partial_u^{l-1} \partial_u \Psi_0^{(o,e)}, \quad V_-^{(-l),(o,e)} = \mp N_l^V \partial_u^{l-1} \partial_v \Psi_0^{(o,e)}, \tag{7}$$

where $N_l^V = \left(-w_0\right)^l$, $l \geq 1$ stands for the modulus of the vortex topological charge in the RHP beam component. The sign $(-)$ corresponds to the ordinary beam $\mathbf{V}^{(-l),(o)}$. All these beams carry over optical vortices. However, this group of vortex-beams *does not involve a fundamental Gaussian beam* in one of the circularly polarized components. To create such a mode beam let us make use of eqs (2, 4) and write

$$G_+^{(o,e)} = -\int_{\overline{u}}^{\infty} \partial_u \Psi_0^{(o,e)}\, du \tag{8}$$

$$G_-^{(o,e)} = \pm \int_{\overline{u}}^{\infty} \partial_v \Psi_0^{(o,e)}\, du\,. \tag{9}$$

where the sign $(+)$ refers to the ordinary beam $G_-^{(o)}$ while the sign $(-)$ is associated with the extraordinary beam $G_-^{(e)}$. The $G_-^{(o,e)}$ component in eq.(9) has an amplitude singularity

at the axis: $u = v = 0$ [8]. To avoid the amplitude uncertainty we require the only RHP *U*-beam to be at the *z=0* plane: $U_-^{(l)}(x, y, z = 0) = 0$, that is

$$U_+^{(0)} = G_+^{(o)} + G_+^{(e)}, \;\; U_-^{(0)} = G_-^{(o)} + G_-^{(e)}. \qquad (10)$$

The equations (8)-(10) enable us to build the second large *U*-group of the vortex-beams as:

$$U_+^{(l)} = N_l^U \partial_v^l \left(G_+^{(o)} + G_+^{(e)}\right), \;\; U_-^{(l)} = N_l^U \partial_v^l \left(G_-^{(o)} + G_-^{(e)}\right). \qquad (11)$$

where $N_l^U = \left(-w_0\right)^l$. For example, the lowest order beam with a complex amplitudes:

$$U_+^{(0)} = \Psi_{0,}^{(o)} + \Psi_0^{(e)}, \;\; U_-^{(0)} = -\frac{\overline{u}}{\overline{v}}\left[w_0^2 \frac{\sigma_o \Psi_0^{(o)} - \sigma_e \Psi_0^{(e)}}{\overline{u}\,\overline{v}} + \Psi_0^{(o)} - \Psi_0^{(e)} \right] \qquad (12)$$

carries over a centered double-charged optical vortex with $l = +2$ in the LHP component when propagating along the z-axis ($\alpha_o = 0$). Similar to the *V*-group of the singular beams, the second *U*-group carries over the optical vortices in each circularly polarized component (excepting the $U_+^{(0)}$ component) whose topological charges differ to two units. At the same time, the RHP components of the beams of the *V*-group carry over the negatively charged vortices while the vortices of the beams of the *U*-group have positive topological charges. More complex singular beams $\mathbf{V}^{(-l,m)}$ and $\mathbf{U}^{(l,m)}$ with the second radial index m can be derived from eqs (7) and (11) by means of the action of the operator $\hat{M}_m^{(o,e)} = \left(-i z_{o,e}\right)^m m!\; \partial_z^m$ on the initial vectors $\mathbf{V}^{(-l)}$ and $\mathbf{U}^{(l)}$ [8].

Our major requirement to the *V*-beams *is* also that their left hand components at the plane *z=0* vanish: $V_-^{(-l)}(x, y, z = 0) = 0$. It means that the vector functions $\mathbf{V}^{(-l,m)} = \mathbf{V}^{(-l,m),(o)} + \mathbf{V}^{(-l,m),(e)}$ together with $\mathbf{U}^{(l,m)} = \mathbf{U}^{(l,m),(o)} + \mathbf{U}^{(l,m),(e)}$ define unambiguously the crystal traveling beams. It permits also us to form the arbitrary beam field **E** at the plane *z=0* with a complex amplitude **W** in terms of the crystal-traveling beams $\mathbf{U}^{(l,m)}$ and $\mathbf{V}^{(-l,m)}$ as:

$$\mathbf{W}(x, y, z = 0) = \sum_{l,m}\left[a_{l,m}\mathbf{V}^{(-l,m)}(x, y, z = 0) + b_{l,m}\mathbf{U}^{(l,m)}(x, y, z = 0)\right], \quad (13)$$

where $a_{l,m}$ and $b_{l,m}$ are the expansion coefficients. In our further consideration we restrict ourselves only to the vortex-beams with a zero radial index *m=0*. Besides, the above requirement enables us to obtain the relation between the angles α_o and α_e [18]: $k_o \alpha_o^2 z_o = k_e \alpha_e^2 z_e$,

II.2 Structural transformations in the tilted vortex-beams

The most intriguing feature of the tilted beams (the beams with complex variable $\overline{y} = y + i\alpha_o z_o$) of the *V*- and *U*-groups is that the optical vortex does not follow the

beam axis. For example, the ordinary vortex beams of the *V*-group derived from eqs (6, 7) have the RHP component in the form

$$V_{+}^{(-l),(o)} = \left[\frac{x - i\left(y + i\alpha_o z_o\right)}{w_0\sigma_o}\right]^l \frac{\exp\left[-\dfrac{x^2+\bar{y}^2}{w_0^2\sigma_o} - k_o\dfrac{\alpha_o^2}{2}z_o\right]}{\sigma_o}. \qquad (14)$$

The Gaussian envelope has a maximum at the point $x = 0$, $y = \alpha_o z$ while the vortex is positioned at the point: $y = 0$, $x = -\alpha_o z_o$. The vortex leaves the axis when tilting the beam. In order to force the vortex to follow the beam it is necessary to construct a new beam

$$V_{+}^{\prime(-l),(o)} = \left[\frac{x - i\left(y - \alpha_o z\right)}{w_0\sigma_o}\right]^l \frac{\exp\left[-\dfrac{x^2+\bar{y}^2}{w_0^2\sigma_o} - k_o\dfrac{\alpha_o^2}{2}z_o\right]}{\sigma_o} \qquad (15)$$

in terms of the crystal-traveling beams. Since

$$\left[\frac{x - i\left(y - \alpha_o z\right)}{w_0\sigma_o}\right]^l \Psi_0^{(o)} = \left[\frac{x - i\left(y - \alpha_o z + i\alpha_o z_o - i\alpha_o z_o\right)}{w_0\sigma_o}\right]^l \Psi_0^{(o)} =$$

$$= \left[\frac{x - i\left(y + i\alpha_o z_o\right)}{w_0\sigma_o} - \frac{\alpha_o z_o}{w_0}\right]^l \Psi_0^{(o)},$$

consequently, the equation (15) is a solution to the paraxial wave equation or otherwise

$$V_{+}^{\prime(-l),(o)} = \sum_{p=0}^{l}\binom{l}{p}\left(-\frac{\alpha_o z_o}{w_0}\right)^{l-p}\left[\frac{x - i\left(y + i\alpha_o z_o\right)}{w_0\sigma_o}\right]^p \Psi_0^{(o)}. \qquad (16)$$

i.e. the RHP component of the tilted beam represents a superposition of elementary beams with a complex $\bar{y}$ variable. By the similar way we can write the beam components $V_{+}^{\prime(-l),(e)}$, $U_{+}^{\prime(l),(o)}$, $U_{+}^{\prime(l),(e)}$. Then with the help of the expressions (7) and (11) we build the LHP components $V_{-}^{\prime(-l),(o)}$, $V_{-}^{\prime(-l),(e)}$, $U_{-}^{\prime(l),(o)}$, $U_{-}^{\prime(l),(e)}$ and the fields $\mathbf{V}^{(-l)}$ and $\mathbf{U}^{(l)}$ of the crystal-traveling beams. The new beam field $V_{+}^{\prime(-l)}$ comprises not only the field of the first *V*-group but also the beam of the second *U*-group (see the term with *p=0* in eq. (16)) whereas the beams $U_{+}^{\prime(l)}$ are defined only by the elementary beams of the *U*-group. Thus, by using expressions (7) and (11) we can write a total rule for constructing the tilted vortex beams in a uniaxial crystal.

$$V_{+}^{(-l)} = \left[\frac{x - i\left(y - \alpha_o z\right)}{w_0\sigma_o}\right]^l \Psi_0^{(o)} + \left[\frac{x - i\left(y - \alpha_e z\right)}{w_0\sigma_e}\right]^l \Psi_0^{(e)}, \ \left(l \neq 0\right) \qquad (17)$$

$$V_{-}^{(-l)} = -N_l^V \sum_{p=1}^{l}\binom{l}{p}\left(-\frac{\alpha_o z_o}{w_0}\right)^{l-p} \partial_u^{p-1}\left(\partial_v \Psi_0^{(o)} - \partial_v \Psi_0^{(e)}\right) + \left(-\frac{\alpha_o z_o}{w_0}\right)^l U_{-}^{(0)} \left(l \neq 0\right) \qquad (18)$$

$$U_{+}^{(l)} = \left[\frac{x + i\left(y - \alpha_o z\right)}{w_0 \sigma_o}\right]^l \Psi_0^{(o)} + \left[\frac{x + i\left(y - \alpha_e z\right)}{w_0 \sigma_e}\right]^l \Psi_0^{(e)}, \tag{19}$$

$$U_{-}^{(l)} = N_l^U \sum_{p=0}^{l} \binom{l}{p} \left(\frac{\alpha_o z_o}{w_0}\right)^{l-p} \partial_v^p \left(G_{-}^{(o)} + G_{-}^{(e)}\right). \tag{20}$$

Without loss of generality, for our theoretical analysis, we choose the initial vortex beams of the *V*- and *U*-groups with topological charges $l_V^+ = -3$ and $l_U^+ = +3$, respectively, in the RHP component at the *z=0* plane. As the vortex beam spreads along the crystal provided that $\alpha_o = const$ (or when changing the angle α_o but $z = const$), the beam field experiences inner reconstruction. The essence of such a structural transformation illustrates Fig.2 and Fig.3.

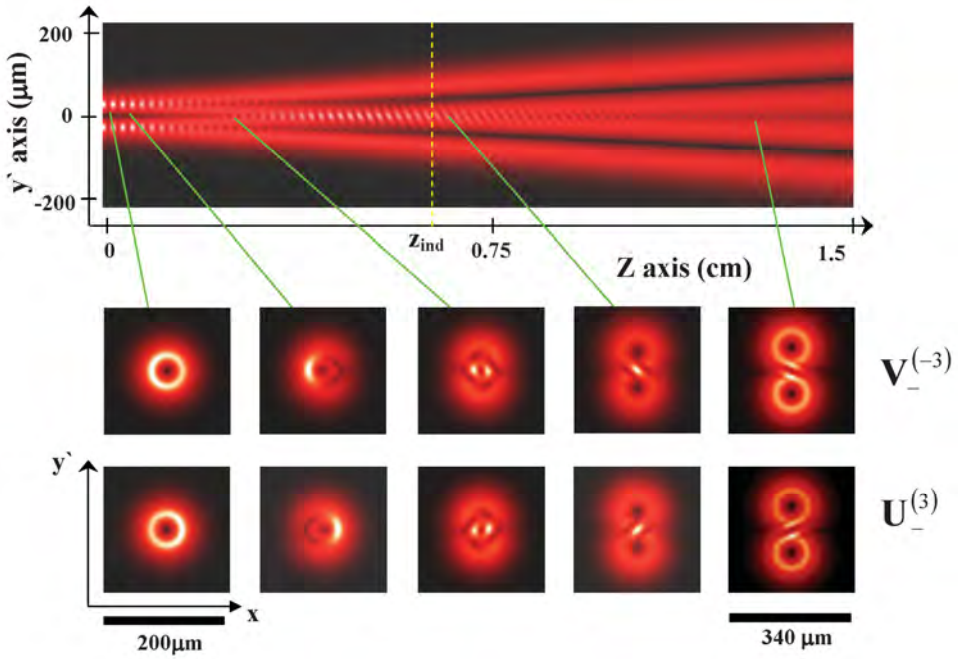

Fig. 2. Splintering of the $V_{-}^{(-3)}$ and $U_{-}^{(3)}$ beam components at the inclination angle $\alpha_o = 10^o$ and $w_0 = 30\,\mu m$. The upper figure is the longitudinal section of the $V_{+}^{(-3)}$ beam component.

Typical patterns of the intensity distributions for different crystal lengths *z* at the given inclination angle α_o for the LHP components $V_{-}^{(-3)}$ and $U_{-}^{(3)}$ are shown in Fig.2

while the vortex trajectories: $\mathrm{Re}\left[V_{-}^{(-3)}\left(x,y,z=const,\alpha\right)\right]=0$, $\mathrm{Im}\left[V_{-}^{(-3)}\left(x,y,z=const,\alpha\right)\right]=0$ in the space $\left\{x,y,\alpha_o\right\}$ are shown in Fig.3.

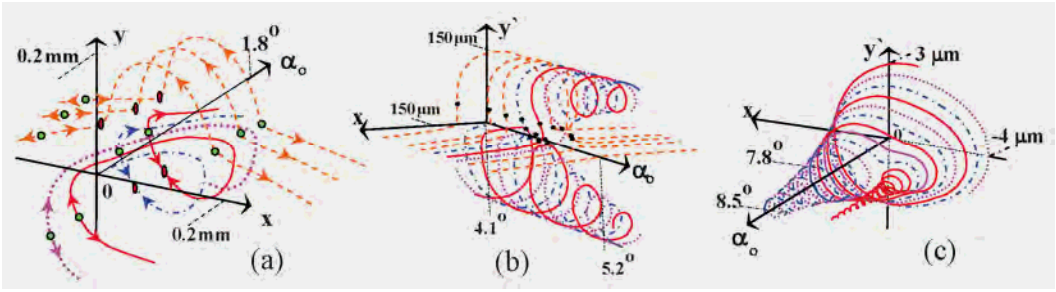

Fig. 3. The key fragments of the vortex trajectories in the $V_{-}^{(-3)}$ beam with $w_0=50\,\mu m$ in the $LiNbO_3$ crystal, $z=2\,cm$.

The reconstruction process has three key fragments: 1) the range of the crystal lengths near $\alpha_o=0$, 2) the range near $\alpha_o=\alpha_{ind}$ (or $z=z_{ind}$) and 3) the range near $\alpha_o=\alpha_{vs}$ (or $z=z_{vs}$). The first initial range $\alpha_o\approx 0$ is characterized by a transition of the beam from the symmetric state when $\alpha_o=0$ into an asymmetric one when $\alpha_o\neq 0$. The LHP component of the $V_{-}^{(-3)}$ beam has the topological charges: $l_V^-=-1$(the charge of the $U_{-}^{(3)}$ beam is $l_U^-=5$) for $\alpha_o=0$) [8].

However, even a very small beam inclination $\left(\alpha_o\neq 0\right)$ destroys fairly rapidly such a vortex state and a total topological charge in the LHP component goes to the charge in the right hand component. This beam reconstruction is accompanied by dislocation reaction shown in Fig.3a. Near the beam axis, two pairs of optical vortices are born. Two negatively charged vortices follow the beam axis alongside with the initial vortex (that results ultimately in recovering the high-order optical vortex) while another pair of the positively charged vortices leaves the beam (red line and dots crimson trajectories at the figures; the blue dash-and-dot color line indicates the initial vortex). When enlarging the angle α_o, the intense dislocation reactions get started. There are two types of the trajectories in the process: the major trunk and the transverse branches (the brick-red dash lines). The positions of the birth and annihilation events are indicated by the green circlets and dark-red ovals, respectively. These two types of the trajectories are not intersected up to the critical angle $\alpha_o=\alpha_{ind}$ (or the critical crystal length $z=z_{ind}$). The processes in the intermediate range are described at length both in the terms of the scalar [18] and the vector [19, 23] singularities. Note that although a simple model of two linearly polarized beams with centered optical vortices presented in the papers [19, 23] describes fairly good the processes in the intermediate range of the inclination angles α_o, it dos not involve the

degenerate case $\alpha_o = 0$ and, consequently, could not take into account the process of the asymmetric recovery of the high-order optical vortices (or polarization singularities) that we will consider later on.

The critical angle $\alpha_o = \alpha_{ind}$ (or $z = z_{ind}$ in Fig.2) corresponds to splitting the beam into two ones: ordinary and extraordinary beams. Noteworthy that not all beams can be splintered but only those that can overcome the border $\alpha_o = \alpha_{ind}$ (or $z = z_{ind}$) for the beam and crystal parameters (so-called the indistinguishability border [24]). In the vicinity of the plane $\alpha_o = \alpha_{ind}$ (or $z=z_{ind}$) three transverse vortex trajectories are bent shaping the core of the second segregated vortex-beam (see Fig.3b). From now on *the vortices on these trajectories in the both splintered beams leave the zone of the dislocation reactions transmitting along screw-like lines without dislocation reactions*. However, the beam deformation caused by the further inclination of the beam stimulates pressing one of the vortex trajectory out of the major trunk of the LHP polarized component (see Fig.3c) while all vortices in the RHP component propagate inside the same trunk. Such an unequal asymptotic behavior of RHP and LHP components derived from the solution to the parabolic wave equation (1) found a simple explanation in terms of the conservation law of the angular momentum flux that will be considered in the next Section.

Let us estimate the asymptotic behavior of the vortices in the $V_{+}^{(-l)}$ and $V_{-}^{(-l)}$ components. We will assume that the ordinary and extraordinary beams in this component are completely split and the beams do not interfere with each other, i.e. $\alpha_o z / w_0, \alpha_e z / w_0 >> 1$. Besides, we will treat the partial beam near its axis so that $\left| x / Z_{o,e} \right|, \left| (y - \alpha_{o,e} z) / Z_{o,e} \right| << 1$, and $Z_{o,e} = z + i\, z_{o,e}$, $y'_{o,e} = y - \alpha_{o,e} z$,

$$\left[\frac{1}{x^2 + \left(y + i\alpha_o z_o \right)^2} \right]_{o,e} \approx -\frac{1}{\left(\alpha_{o,e} Z_{o,e} \right)^2} \sum_{q=0}^{l} (-1)^q \left(\frac{r'^2_{o,e}}{\alpha^2_{o,e} Z^2_{o,e}} + 2i \frac{y'_{o,e}}{\alpha_{o,e} Z_{o,e}} \right)^q ,$$

$$\left(\frac{\overline{u}}{\overline{v}} \right)_{o,e} \approx -\left[1 - \frac{i}{\alpha_{o,e} Z_{o,e}} \left(x + i\, y'_{o,e} \right) \right]^p \times \sum_{p=0}^{l} \left(\frac{-i}{\alpha_{o,e} Z_{o,e}} \right)^p \left(x - i\, y'_{o,e} \right),$$

where $r'^2_{o,e} = x^2 + y'^2_{o,e}$. In the above equations, we restricted ourselves to the *l*-th term in the power series associated with a topological charge l of the considered vortex-beam. Besides, the value $\overline{r}^2 = x^2 + \left(y + i\alpha_o z_o \right)^2$ does not depends on the $o-$ or $e-$ indices in the complex beam because $\alpha_o z_o = \alpha_e z_e$. However, it is necessary to take into account these indices in the radius $r'_{o,e}$ when considering each partial beam separately. After a tedious but straightforward algebra in the expressions (23) and (24) we come to the asymptotic expressions for the $V_{+}^{(-l),(o)}$ and $V_{-}^{(-l),(o)}$ components:

$$V_{+}^{(-l),o} \propto \left(\frac{x - i\, y'_o}{w_0 z / z_o} \right)^{l} \Psi_0^{(o)}, \tag{21}$$

$$V_{-}^{(-l),o} \propto \left(\frac{x - i\, y'_o}{w_0 z / z_o} \right)^{l-1} \left(\frac{z_o}{w_0 z} \right) \left(\frac{2l}{\alpha_o k_o} + x - i\, y'_o \right) \Psi_0^{(o)}. \tag{22}$$

Similarly we can obtain the asymptotic expressions for the extraordinary $V_{+}^{(-l),(e)}$ and $V_{-}^{(-l),(e)}$ partial beams Thus, the $V_{+}^{\prime(-l)}$ component has two branches of the ordinary and extraordinary beams with centered *l*-order optical vortices. The $V_{-}^{\prime(-l)}$ component has also two branches. However, the vortices have a complex structure. They do not gather together at the axis like those in the ordinary beam. The vortices of the *l*-1 order are positioned at the axes of the beams: $x_1^{(o)} = 0$, $y_1^{(o)} = \alpha_o z$ and $x_1^{(e)} = 0$, $y_1^{(e)} = \alpha_e z$. The second pair of vortices with unit topological charges is shifted along the x-axis at the distance $\Delta x_V = -2l/(\alpha_o k_o)$ relative to their neighbors in the V_{+} beam component: $x_2^{(o)} = -2l/(\alpha_o k_o)$, $y_2^{(o)} = \alpha_o z$ and $x_2^{(e)} = -2l/(\alpha_o k_o)$, $y_2^{(e)} = \alpha_e z$. The magnitude of the transversal vortex shift Δx increase linearly with growing the vortex topological charge l and does not depend on the crystal length z. It means that the extraordinary beam do not recover its initial structure at any crystal length. It lead to a drastic consequence.

Indeed, in frameworks of the model of two linearly polarized tilted beams [19, 23] with centered optical vortices, the superposition of the circularly polarized beam components in the asymptotic case must form a total beam with a uniformly distributed linear polarization over cross-sections of the splintered partial beams, the linear polarizations being orthogonal to each other in these beams. However, a complex vortex structure in each polarized component of a total wave field (17-20) derived from the paraxial wave equation (1) results in a non-uniformly polarized field distribution in the vicinity of the beam core. This situation is shown in Fig.4.

The polarization distribution represents a set of polarization ellipses on the background of the polarization ellipticity $Q = \pm b/a$ (*a* and *b* is the ellipse axes). The solid lines (streamlines) are oriented along the major axes of the ellipses that are characterized by inclination angle ψ to the x-axis [12]. The streamlines trace the characteristic pattern in the vicinity of the C-points – the points of the polarization singularity. One of the circularly polarized components vanishes at this point. In fact, the C-point characterizes the vortex position in one of the field components. There are three types of patterns traced by the streamlines: the star, the lemon and the monstar. The star is characterized by the topological index $\nu = -1/2$ whereas the lemon and the monstar have the same topological indices $\nu = +1/2$. The picture in Fig.4b has six characteristic patterns: three stars and three lemons for the one of the beams of the *V*-group at the inclination angle $\alpha_o = 8^o$. As the angle α_o increases, three lemons and two stars draw together forming the pattern with a topological index

$\nu = -1/2 - 1/2 + 1/2 + 1/2 + 1/2 = +1/2$ that we classify as a degenerated lemon (see Fig. 4c). This polarization singularity corresponds to the position of the double negatively charged optical vortex in the $V_{-}^{(3)}$ component and the triple negatively charged vortex in the $V_{+}^{(-3)}$ component. The star shifted relative to the lemon corresponds to the singly charged vortex in the $V_{-}^{(-3)}$ component. The computer simulation showed that these polarization singularities are always separated at any crystal lengths.

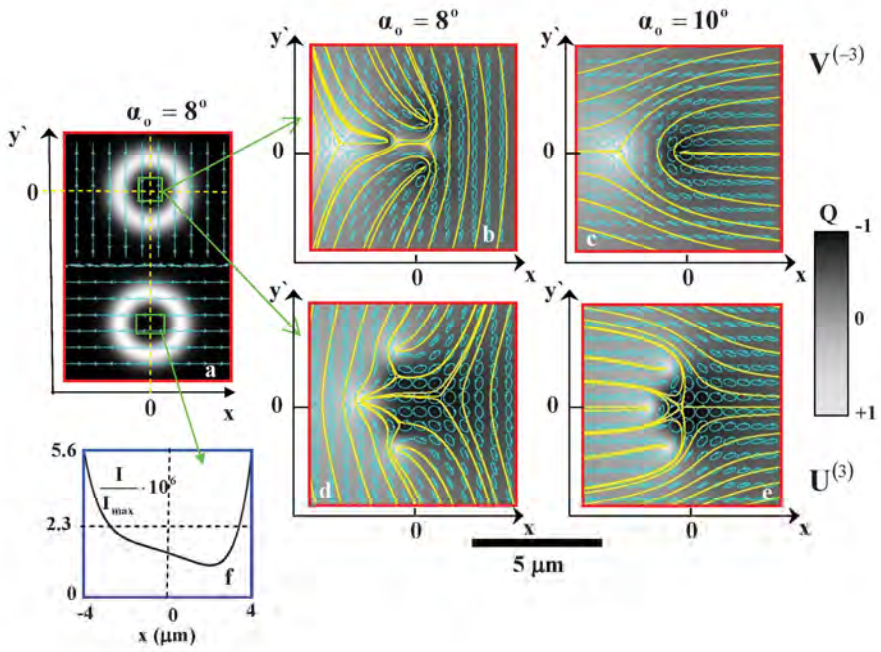

Fig. 4. Polarization distribution; $n_1 = 2.3$, $n_3 = 2.2$, $z = 2\,cm$, $w_0 = 30\,\mu m$; (a) the intensity distribution in the vicinity of the $\mathbf{V}^{(-3)}$ beam core, (b), (c) polarization singularities for $\mathbf{V}^{(-3)}$ and (d), (e) $\mathbf{U}^{(3)}$ beams, (f) the intensity profile in the vicinity of the $\mathbf{V}^{(-3)}$ beam.

The absolutely other situation is observed for the polarization singularities in the *U*-beam group. The fact is that in the case of the $U_{-}^{(3)}$ beam, two vortices in the orthogonal component leave the vortex-beam at the very beginning of the dislocation reactions $\alpha_o \approx 0$ so that ultimately the splintered beams recover also a total topological charge $l = 3$ for $\alpha_o > \alpha_{ind}$. However, the vortices do not gather together but form asymmetric composition shifted along the x-axis. The picture in Fig. 4d represents also a complex combination of three lemons and three stars at the angle $\alpha_o = 8^o$. When further

increasing the angle α_o, three stars gather together at the point $x = 0,\ y' = 0$ forming a degenerated polarization singularity with a topological index $\nu = -3/2$ (Fig. 4e). However, the rest three lemons form something like an asymmetric vortex-cloud shifted along the *x*-axis in the vicinity of the central point. Such a vortex structure does not change while growing the crystal length. The growth of the topological charge $|l|$ of the initial beam entails a linear displacement of the lateral C points along the *x*-axis for both the *V*- and *U*-groups of the beams.

Before studying the influence of the handedness of a circular polarization and a sign of the vortex topological charge on the transverse shift of optical vortices, let us note that the beam fields presented by the expressions (17)-(20) are not the only ones. We can construct new groups of fields with the help of changing the variable of differentiation and integration from $\overline{u}$ to $\overline{v}$ in eqs (11), (15) and (12), (13). Then the equations (11) and (15) can be rewritten in the form:

$$V_+^{(l),(o,e)} = \mp N_l^V \partial_v^{l-1} \partial_u \Psi_0^{(o,e)},\ V_-^{(l),(o,e)} = N_l^V \partial_v^{l-1} \partial_v \Psi_0^{(o,e)}, \tag{23}$$

$$\overline{U}_+^{(-l)} = N_l^U \partial_u^l \left(\overline{G}_+^{(o)} + \overline{G}_+^{(e)}\right),\ \overline{U}_-^{(-l)} = N_l^U \partial_u^l \left(\overline{G}_-^{(o)} + \overline{G}_-^{(e)}\right), \tag{24}$$

where $\overline{G}_+^{(o,e)} = \pm\int_{\overline{v}}^{\infty} \partial_u \Psi_0^{(o,e)}\, dv$, $\overline{G}_-^{(o,e)} = -\int_{\overline{v}}^{\infty} \partial_v \Psi_0^{(o,e)}\, dv$.

Besides, our requirement is now: the RHP component of the initial field vanishes at the z=0 plane: $\overline{V}_+(x, y, z = 0) = 0$, $\overline{U}_+(x, y, z = 0) = 0$. Then, the beam components get the form:

$$\overline{V}_+^{(l)} = -N_l^V \sum_{p=1}^{l} \binom{l}{p} \left(\frac{\alpha_o z_o}{w_0}\right)^{l-p} \partial_v^{p-1} \times \left(\partial_u \Psi_0^{(o)} - \partial_u \Psi_0^{(e)}\right) + \left(\frac{\alpha_o z_o}{w_0}\right)^{l} \overline{U}_+^{(0)};\ (l \neq 0) \tag{25}$$

$$\overline{V}_-^{(l)} = \left[\frac{x + i\left(y - \alpha_o z\right)}{w_0 \sigma_o}\right]^l \Psi_0^{(o)} + \left[\frac{x + i\left(y - \alpha_e z\right)}{w_0 \sigma_e}\right]^l \Psi_0^{(e)}\ (l \neq 0) \tag{26}$$

$$\overline{U}_+^{(-l)} = N_l^U \sum_{p=0}^{l} \binom{l}{p} \left(-\frac{\alpha_o z_o}{w_0}\right)^{l-p} \partial_u^p \left(\overline{G}_+^{(o)} + \overline{G}_+^{(e)}\right), \tag{27}$$

$$\overline{U}_-^{(-l)} = \left[\frac{x - i\left(y - \alpha_o z\right)}{w_0 \sigma_o}\right]^l \Psi_0^{(o)} + \left[\frac{x - i\left(y - \alpha_e z\right)}{w_0 \sigma_e}\right]^l \Psi_0^{(e)}. \tag{28}$$

The LHP component of the *V*-group of the initial beams carries over positively charged vortices whiles the *U*-group – negatively charged ones. *Comparing with the field (17)-(20) we can infer that the handedness of the circular polarization of the beams and the vortex topological charges are tightly bound with each other in the crystal-traveling beams*. Computer simulation showed that the directions of the vortex transversal shift both in *V*- and *U*-groups *are exclusively defined by the handedness of the initial circular polarization*. Otherwise, the vortex transversal shift has the same direction for the *V*-beam group with the RHP and the $l < 0$ topological charge and the *U*-beam group with the

RHP and the $l > 0$ topological charge (just as for the $\overline{V}$ -beam group with the LHP and $l > 0$ and the $\overline{U}$ -beam group with the LHP and $l < 0$).

Linearly polarized vortex-beams represent superposition of the circularly polarized ones: $\mathbf{F}_X^{(-l)} = \mathbf{V}^{(-l)} + \overline{\mathbf{U}}^{(-l)}$ and $\mathbf{F}_Y^{(-l)} = -i(\mathbf{V}^{(-l)} - \overline{\mathbf{U}}^{(-l)})$. Naturally, these vortex-beams are non-uniformly polarized near the beam core in the asymptotic case. Fig. 5 illustrates behavior of the polarization singularities inside the core of the vortex beam $\mathbf{F}_X^{(-3)}$ after splitting. At the inclination angle $\alpha_o = 7^o$, three lemons and three stars are grouped around the beam axis. As the angle α_o increases, two stars flow together forming a degenerated star at the beam axis $y' = 0, x = 0$ at the angle $\alpha_o = 10^o$ while the asymmetric cloud of three lemons are shifted to the left and one star is shifted to the right. Thus, a magnitude of the relative shift between the polarization singularities is doubled. In the RHP components, we will observe the cloud of optical vortices shifted to the left whereas the LHP component comprises the centered double-charged vortex and one singly-charged vortex shifted to the right.

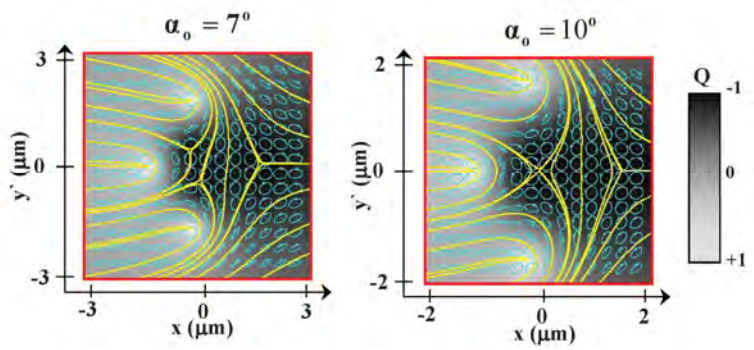

Fig. 5. Polarization singularities inside the core of the $\mathbf{F}_X^{(-3)}$ beam: z=2 cm, w_0=30 μm.

II.3 The experiment

A series of nontrivial theoretical results described above needs an experimental basis. First of all, this relates to a different behavior of RHP and LHP components in the splintered beams that results in a non-uniformly polarized field distribution in the vicinity of the beam core. It is important to note that the polarization heterogeneity of the paraxial beams split by the uniaxial crystal is inherent in all singular beams irrespective of a magnitude of their topological charges. Although the area of the polarization inhomogeneity increases when growing the vortex topological charge *l*, light intensity decreases very quickly in this area. Besides, a high-order optical vortex embedded in the beam is of an unstable structure that can be destroyed by a very small external perturbation [25]. Naturally, experimental measurements with off-axis high order vortex-beams transmitting through a series of boundary faces of the optical elements in the real experimental set-up are accompanied by a very high experimental error. As a result, we

restricted ourselves to the experiments with singly charged vortex-beams. In the article [18], we have experimentally considered the vortex-beam behavior in a uniaxial crystal in the vicinity of the indistinguishability boarder $\alpha_o = \alpha_{ind}$ (or $z = z_{ind}$) [24]. In the given section, we will focus our attention on the beam structure far from this border when the beams are separated and their mutual interference vanishes. We will concentrate ourselves on the transformations of the C-lines in the vicinity of the beam core.

The sketch of the experimental set-up is shown in Fig.6. The non-singular beam from the Ne-Ne laser $(\lambda = 0.6328\mu m)$ is transformed into a vortex-beam with a topological charge $l = \pm 1$ by a computer generated hologram (Tr). Diffraction orders after the computer generated hologram are clearing by the diaphragm (D). The polarizer (Pol) and the quarter-wave retarder ($\lambda/4$) insert a circular polarization into the beam. The handedness of the circular polarization is defined by the direction of the axes of the $\lambda/4$ plate and can be converted into opposite one by a simple rotation of the $\lambda/4$ plate axes at the angle 90^o. Further the beam is focused by a lens (L) with the focal length $f = 5cm$ into the $LiNbO_3$ crystal at the angle α_{in} to the crystal optical axis **C** (the crystal length is about z=2 cm).

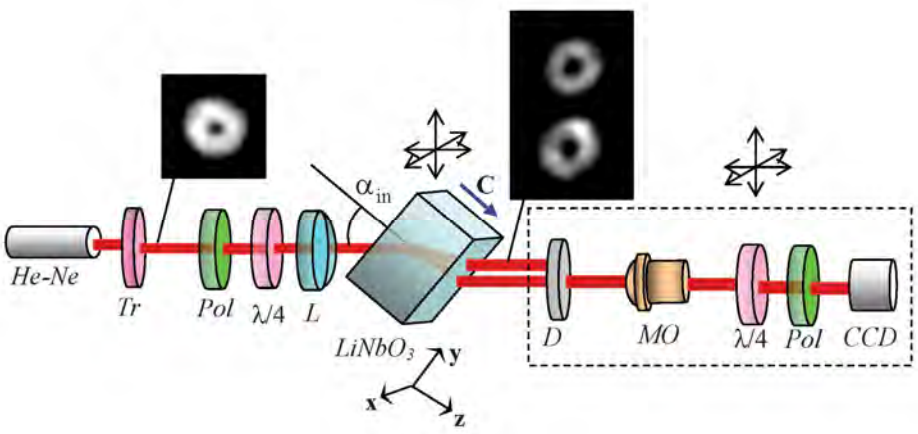

Fig. 6. The sketch of the experimental set-up: (He-Ne) – laser, (Tr) – computer-generated hologram, (Pol) – polarizer, $\lambda/4$ - quarter-wave retarder, (L) – lens with f=5 cm, ($LiNbO_3$) – crystal, (D)- diaphragm, (MO) – 20^x microobjective; (CCD) –CCD camera.

The crystal is positioned on a rotary table that enables us to rotate the crystal with the angle precision about 0.03^o. The beam after the crystal is collimated by the diaphragm (D) and 20^x microobjective (MO). After passing through a quarter-wave retarder and the polarizer, the beam is detected by the CCD camera. The optical elements positioned after the crystal are mounted on the special 3D-optical table that permits us to tune up the beam image at the CCD camera after rotating the crystal. We could measure the specific Stokes parameters at each pixel of the beam image at the CCD camera in accordance with a

standard technique [7, 18]. The spatial resolution in the beam image was about $1.5\,\mu m$. The position of the origin on the x-y plane is defined as a center of gravity of the beam at the CCD camera plane for each angle α_{in} to within $1.7\,\mu m$ provided that the initial beam is a linearly polarized. The described above technique does not permit us to measure a magnitude of the asymptotic transverse shift of the vortices Δx_V (see Sections II).

Nevertheless, we can study experimentally major features of the fine polarization structure of the beam core and bring to light major tendencies of the vortex-beam behavior in each circularly polarized component when tilting the beam. We measured the positions x and y of the C-points for each angle α_{in} within to $1.5\,\mu m$ on the base of standard method [7, 18]. We started to measure the C-point positions at the beam cross-section when the light intensity between the beams was 10 times as small as the intensity at the beam maximum. This corresponds to a rather well splitting of the partial beams. A typical map of the polarization distribution is shown in Fig.7.

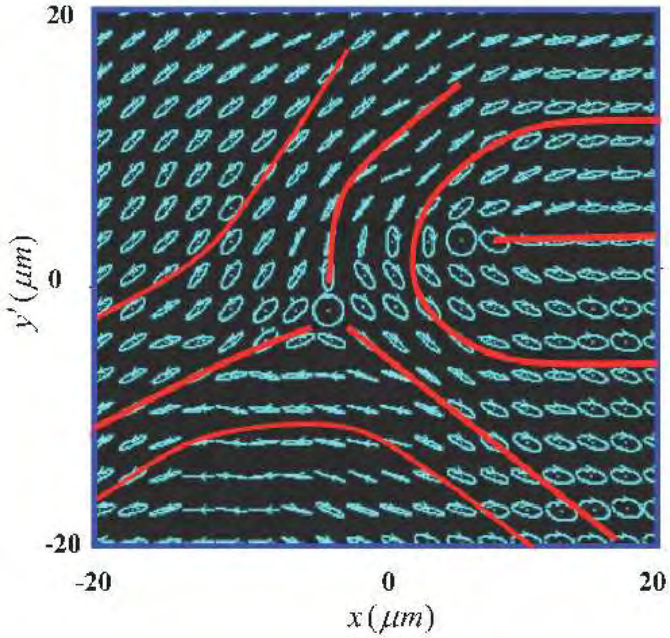

Fig. 7. Map of the polarization distribution in the vicinity of the beam core with the initial RHP polarization and $l = -1$.

We can see here standard patterns of the star and the lemon around the C-points. When tilting the beam, the C-points start to rotate and a distance between them changes. Their positions trace a complex trajectories in the space: x, y, α_{in}. At first, we plotted trajectories traced by the lemon and the star inside the core of the ordinary singular beam with a right hand circular polarization and a negative topological charge $l = -1$ at the input crystal face shown in Fig.8 (the lower partial beam in the Fig.6). The star is

associated with a vortex in the RHP component whereas the lemon corresponds to the vortex in the LHP component. They move along spiral-like trajectories. The radii of their rotation decrease gradually. Note that the handedness of the C-line rotations is the same. (However, the handedness of both trajectories changes its sign in the extraordinary beams propagating at the angle α_e (the upper partial beam in the Fig.6)). The star is rotated around the α_o axis while the axis of rotation of the lemon is asymptotically approach to the axis of rotation of the star. After the angle $\alpha_{in} \approx 12^o$, the trajectories draw together at the distance lesser than $2\mu m$ and are experimentally perceived as one line. When changing a sign of the initial circular polarization to the opposite one, the star and the lemon in Fig. 7 are transposed. The lemon is moved now along a spiral-like trajectory rotating around the α_o axis. The trajectory of the star is shifted to the positive direction of the x-axis approaching gradually to the trajectory of the lemon. The switching of a sign of the initial vortex to the opposite one does not change essentially the form of the C-lines. Thus, the direction of the transverse shift of the vortices is exceptionally defined by a handedness of the initial circular polarization. At the other hand, the direction of the transverse shift of the vortices changes to the opposite one when changing the sign of the inclination angle α_o.

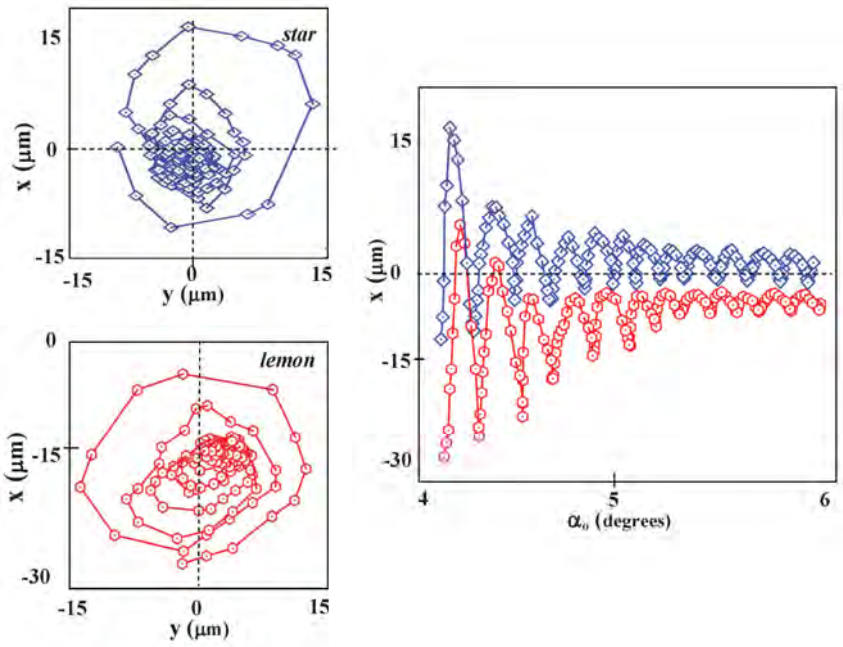

Fig. 8. C-lines for the RHP initial beam with l=-1, $w_0 \approx 50\mu m$, $z \approx 2cm$.

For comparison, we introduce theoretical trajectories in Fig.9 plotted for much the same parameters of the beam and the crystal. (The equation for the C-lines is derived from

the requirement: the first and the second specific Stokes parameters vanish or $s_1(x,y,z,\alpha_o) = E_+E_-^* + E_+^*E_- = 0$, $s_2(x,y,z,\alpha_o) = i\left(E_+E_-^* - E_+^*E_-\right) = 0)$. The theoretical C-lines for the $\mathbf{V}^{(-)}$-beam in Fig.9 also have all major features of the experimentally observed trajectories and are in a good qualitative agreement with the experimental curves in Fig.8. The behavior of the lemon and the star in the initially *x*-linearly polarized beam $\mathbf{F}_x$ is shown in Fig.10. The C-lines have also a spiral-like form. However, both trajectories are symmetrically shifted along the positive and negative directions of the x-axis. In contrast to the circularly polarized $\mathbf{V}^{(-)}$-beam, the tilted linearly polarized $\mathbf{F}_x$ beam has a vanishingly small intensity of the orthogonal component. As a result, the interference between the ordinary and extraordinary beams is experimentally observed only for very small inclination angles. The C-lines of the linearly polarized $\mathbf{F}_x$ beam oscillates much slower and approach to each other very quickly. Nevertheless, we observe distinctly two trajectories drawing together with relatively slow oscillations. After the angle $\alpha_{in} \approx 7^o$, the trajectories are experimentally undistinguished and we cannot judge about their asymptotic behavior. Comparison of the curves in Fig.9 for the $\mathbf{F}_x$ and Fig.10 shows their good qualitative agreement.

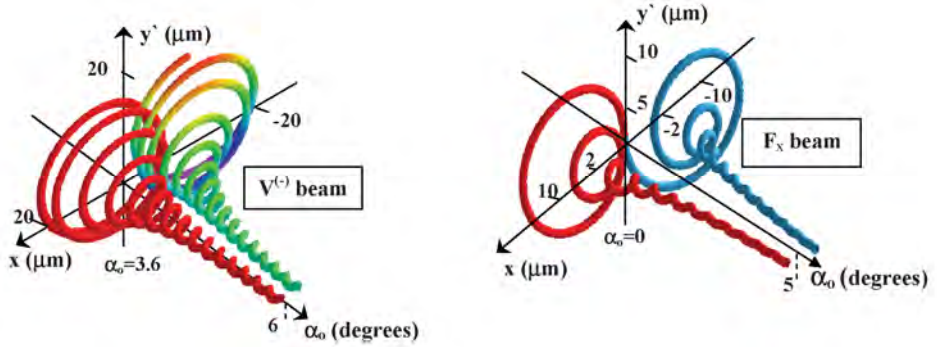

Fig. 9. A computer simulation of the C-line behavior in the $\mathbf{V}^{(-)}$ and $\mathbf{L}_x$ beams, $l = 1$.

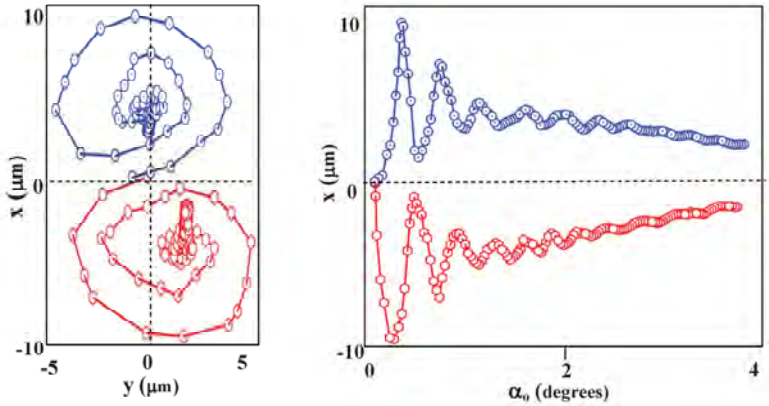

Fig. 10. C-lines in the *L*-beam with: $l = -1$, $w_0 \approx 50\,\mu m$, $z \approx 2\,cm$.

The vortex transverse shift in the singular beams stimulates inevitably the transverse shift of the circularly polarized beam components and distortion of their cross-sections.

III THE TRANSVERSE SHIFT, ANGULAR MOMENTUM AND DEFORMATION OF THE BEAM CROSS-SECTION

III.1 The angular momentum

Generally speaking, the conservation law of the angular momentum of light in a simple form as a sum of the SAM and OAM for homogeneous isotropic media [15] cannot be employed in an anisotropic medium because the anisotropic crystal has sources and sinks of the angular momentum of light [26]. It means that the angular momentum of light can be coupled with the angular momentum of the medium. Nevertheless, Ciattoni et al. [16] showed that, in the paraxial approximation, the conservation law can be written for the component of the total angular momentum flux along the optical axis of the uniaxial crystal where the medium is rotationally invariant and the coupling between the angular momentum of the medium and light vanishes. The balance equation can be written in the form:

$$S_z(z) + L_z(z) = I_+ - I_- + L_z^{(+)} + L_z^{(-)} = l + \sigma, \tag{29}$$

where S_z and L_z stand for the spin and orbital angular momenta, respectively, I_+ and I_- are the dimensionless intensities of the RHP and LHP components, $L_z^{(+)}$ and $L_z^{(-)}$ are the OAM of the RHP and LHP components, l and σ are the topological charge and handedness of the beam at the z=0 plane. Although the spin and orbital components of the angular momentum flux can change their magnitudes when transmitting the beam, the spin-orbit coupling [16, 17] forces their sum to remain constant. The beam propagation along the crystal is accompanied by its depolarization, i.e. decreasing of the SAM. The depolarization process in turn "switches on" the spin-orbit coupling so that the OAM get transformed.

Polarization state in the vortex-beam can be considered on the base of the Stokes parameters:

$$S_0 = \Im = \Im_+ + \Im_-,\ S_1 = \int_{-\infty}^{\infty} dx \int_{-\infty}^{\infty} dy \left(E_+ E_-^* + E_+^* E_-\right), \tag{30}$$

$$S_2 = i\int_{-\infty}^{\infty} dx \int_{-\infty}^{\infty} dy \left(E_+ E_-^* - E_+^* E_-\right),\ S_3 = \int_{-\infty}^{\infty} dx \int_{-\infty}^{\infty} dy \left(E_+ E_+^* - E_-^* E_-\right) = \Im_+ - \Im_-, \tag{31}$$

here the symbol $(^*)$ stands for a complex conjugation. $\Im_\pm$ are the normalized intensities of RHP and LHP components, respectively. The magnitude

$$S_z = \frac{S_3}{\Im} = \frac{\Im_+ - \Im_-}{\Im} = I_+ - I_- \tag{32}$$

describes the SAM of the vortex-beam. The polarization degree can be presented as

$$P = \frac{\sqrt{S_1^2 + S_2^2 + S_3^2}}{\Im}. \tag{33}$$

Fig.11 demonstrates behavior of the SAM for the $\mathbf{U}^{(0)}$ and $\mathbf{V}^{(-3)}$ beams. The oscillations of the SAM in the $\mathbf{V}^{(-3)}$ beam die down periodically before vanishing while the oscillations of the vortex-free $\mathbf{U}^{(0)}$ beam decrease monotonically. In both cases the oscillations have envelopes in the form of the polarization degree *P*.

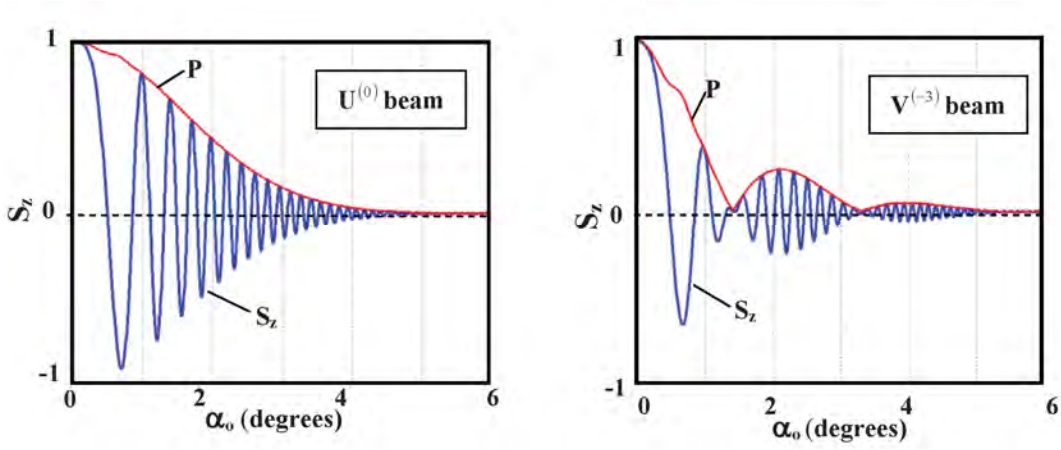

Fig. 11. $S_z(\alpha_o)$ and $P(\alpha_o)$ of the beam $\mathbf{U}^{(0)}$ and t $\mathbf{V}^{(-3)}$ beams, z=2 cm.

The OAM of the paraxial beam L_z is calculated by mean of the expression:

$$L_z = -\frac{i}{\Im}\int_{-\infty}^{\infty} dx \int_{-\infty}^{\infty} d\,y\ \mathbf{E}^* \left(x\,\partial_y \mathbf{E} - y\,\partial_x \mathbf{E}\right), \tag{34}$$

It can be presented as a sum of the OAM of the RHP and LHP beam components $L_z = L_z^+ + L_z^-$. The curves shown in Fig. 12 describe the OAM evolution for the $\mathbf{U}^{(0)}$, $\mathbf{U}^{(3)}$ and $\mathbf{V}^{(-3)}$ beams The $\mathbf{U}^{(3)}$ and $\mathbf{V}^{(-3)}$ beams have opposite signs of the topological charges $l = +3$ and $l = -3$, respectively, and the same handedness of the circular polarization $\sigma = +1$ at the initial plane z=0. All the curves $L_z(\alpha_o)$ oscillate synchronically with the curves $S_z(\alpha_o)$ (see Fig. 11).

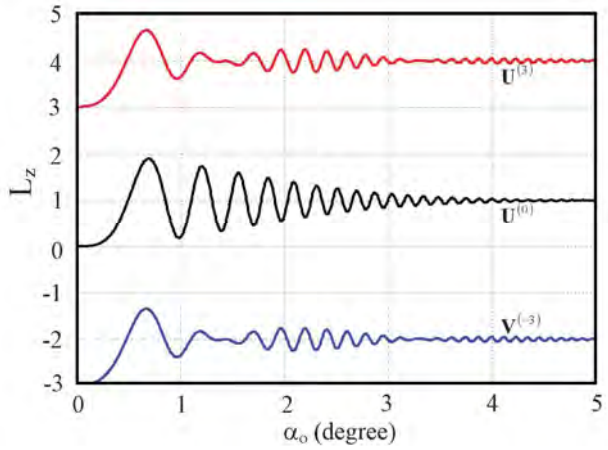

Fig. 12. $L_z(\alpha_o)$ for the $\mathbf{U}^{(3)}$, $\mathbf{U}^{(0)}$ and $\mathbf{V}^{(-3)}$ beams; $w_0 = 50\mu m$, z=2 cm.

However, the sections of the curves in Fig.11 where the SAM increases, corresponds to the section of the curves in Fig. 12 where the OAM decreases and vice versa. At the first sight, it seems that the sum of the topological charge and handedness at the initial plane z=0 and at the asymptotic case $z \to \infty$ must be the same: $l_{in} + \sigma_{in} = l_{asym}$. But a simple estimation shows invalidity of such assumption: $l_{in} + \sigma_{in} \neq l_{asymp}$. Even the vortex-free ($l = 0$) beam $\mathbf{U}^{(0)}$ with a zero initial OAM $L_z(z=0) = 0$ gets the asymptotic orbital angular momentum $L_z^{(asymp)} = +1$ that has nothing to do with the vortex topological charge l. At the same time, the optical vortices are not the only reason that can change the OAM. Considerable contribution to the OAM is also made by the astigmatic transformations [15] and the transverse shift of the center of gravity of the beam as a whole.

III.2 The transverse shift

The brightest example of interrelation between the transverse shift and AM in optical processes is the Fedorov-Imbert effect [27- 32] – the lateral displacement of the beam when refracting or reflecting it at the interface of two homogeneous isotropic media. The basic part in this phenomenon plays the spin-orbit coupling. The transverse shift manifest itself also in the spin Hall effect: the splitting of a linearly polarized beam into two circularly polarized ones [33-35] and in the optical Magnus effect: rotation of the trajectory of a circularly polarized ray in an optical fiber [36, 37]. The singular beams bearing optical vortices enhance noticeably the effect owning to an additional orbital angular momentum associated with the optical vortices [38-40]. Moreover, the direction of the beam shift at the boundary face is defined now not only by the handedness of the circular polarization but also by the sign of the vortex topological charge. The imprescriptible element of the considered above processes is inhomogeneity of the medium. In this Section, we will concentrate our attention on the transverse shift of the beam in the unbounded homogeneous but anisotropic medium.

We calculated the positions of the center of gravity of the beam on the base of the standard expressions:

$$x_C = \frac{1}{\Im}\int_{-\infty}^{\infty} dx \int_{-\infty}^{\infty} d\,y\; x\,\left|\mathbf{E}(x,y,z,\alpha_o)\right|^2 , \quad y_C = \frac{1}{\Im}\int_{-\infty}^{\infty} dx \int_{-\infty}^{\infty} d\,y\; y\,\left|\mathbf{E}(x,y,z,\alpha_o)\right|^2 . \quad (35)$$

The chains of the dislocation reactions in the tilted vortex-beams force the center of gravity trace intricate space trajectories for each of the circularly polarized components. The typical trajectories are shown in Fig. 13 for the $\mathbf{V}^{(-3)}$ vortex-beam. The amplitude of vibrations of the trajectory depends on the crystal length *z* and the inclination angle α_o. The amplitude has large value inside the angle range from $\alpha_o = 0$ to the indistinguishability border $\alpha_o = \alpha_{ind}$. In the vicinity of the value $\alpha_o = \alpha_{ind}$, the vibrations die down because a part of vortices that take place in the reconstruction of the beam core, leaves the area of dislocation reactions. Then the vibrations are resumed again but with essentially smaller amplitude while their frequency increase very much. Finally, the vibrations fade away at the relatively large angles α_o (or the crystal length *z*). However, we observe the residual displacement one of the beams. The position of the center of gravity of the $V_-^{(-3)}$ component is shifted along the x-axis at the distance: $\Delta x^- = -2/(k\,\alpha_o)$ while the shift on the orthogonal plane vanishes $\Delta y^- = 0$. At the same time, the center of gravity of the total beam $\mathbf{V}^{(-3)}$ is shifted only at a half of this distance: $\Delta x_T = \Delta x^- / 2$ while for all that the $V_+^{(-3)}$ component is not shifted. The circularly polarized components of the $\mathbf{F}_X$ beam with the initial linear polarization directed along the *x*-axis and the vortex topological charge *l* are shifted in opposite directions so that in the asymptotic case the transverse shift between circularly polarized components is doubled $\Delta x_C^{(V)} = 4/(k\,\alpha_o)$.

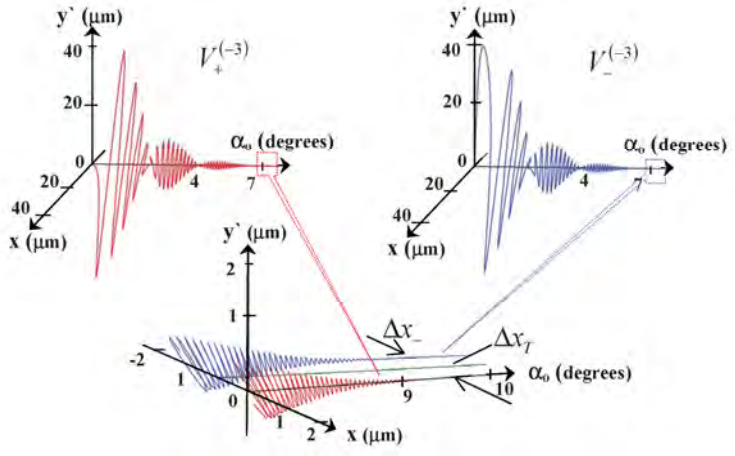

Fig. 13. The trajectories of the center of gravity of the $\mathbf{V}^{(-3)}$ beam; z=2 cm, $w_0 = 50\,\mu m$.

It is noteworthy to remark that the magnitudes of the asymptotic transverse shifts Δx_T of the center of gravity for the circularly polarized components of the $V, U, \overline{V}, \overline{U}$ beams are the same for different magnitudes of the initial vortex topological charges l although the transverse shift of the vortices in these components is proportional to the vortex topological charge l. This result can be independently obtained from the equation (29) for the angular momentum flux.

Let us rewrite the conservation law (29) in the alternative form bound with the evolution of the center of gravity of the beam [29]:

$$\left(\mathbf{r}_c \times \mathbf{k}_c\right)_z + \left(I_+ - I_- + I_+ l_+ + I_- l_-\right)\frac{k_z}{k} = const\,, \tag{36}$$

where $\mathbf{r}_c$ is the radius vector of the center of gravity, k_z stands for the *z*-component of the wave vector of the beam associated with the center of gravity, l_+ and l_- are the vortex topological charges in the RHP and LHP components, respectively. Since the inclination angle is small we can assume that $k_z / k \approx 1$. The first term in eq. (36) is $\left(\mathbf{r}_c \times \mathbf{k}_c\right)_z = -k\alpha_o \Delta x_T$ in the referent frame shown in Fig.1. The sum of the SAM and OAM at the initial plane z=0 is equal to the asymptotic AM flux at the $z \to \infty$, i.e $l + \sigma = \frac{1}{2} l_+ + \frac{1}{2} l_- - k\alpha_o \Delta x_T$. However, the vortex topological charges in the RHP and LHP components equal each other $l_+ = l_- = l$ and the beam is depolarized $\left(I_+ = I_-\right)$ in the asymptotic case so that the transverse shift: $\Delta x_T = -\sigma / k\alpha_o$ is the same for all vortex beams (including the Gaussian beam) and does not depend on the vortex topological charge. The above result derived from the conservation law (36) coincides with the asymptotic value of the transverse shift Δx_T in Fig. 13 obtained from the solution of the paraxial wave equation (1).

Thus, the asymmetric splitting and the transverse shift of the tilted vortex-beams in a uniaxial crystal is a consequence of the conservation law for the total angular momentum flux along the crystal optical axis and manifests itself as a joint action of the dislocation reactions in the circularly polarized components, the beam depolarization and the spin-orbit coupling.

III.3 The deformation of the beam cross-section

The asymmetric vortex destruction and recovery in the paraxial beam considered in Sec. II causes not only the transverse shift but also distortion of a circular symmetry of the beam cross-section. Generally speaking, a uniaxial crystal deforms the initially circular cross-section of the paraxial extraordinary beam when propagating perpendicular to the crystal optical axis [41] even without taking into account the vortex structure of the beam. Complex behavior of such deformation in tilted paraxial beams

was remarked also in the article [3]. A circularly polarized beam propagating along the crystal optical axis does not experience an elliptical deformation. At the same time, a linearly polarized Laguerre-Gaussian beam in this case undergoes a relatively strong deformation, its magnitude increasing as the beam propagates along the crystal [42]. Contribution of the transverse shift to the beam deformation is of the object of a special investigation. However, in the given Section we will consider only some features of such a complex process.

The magnitude of the cross-section deformation can be estimated by means of the *mean square width* of the paraxial beam (see, e.g., [41]):

$$W_{\pm}^2(\varphi, z, \alpha_o, l) = \frac{1}{\Im_{\pm}} \int_{-\infty}^{\infty} d\,x \int_{-\infty}^{\infty} d\,y' \left(x\cos\varphi + y'\sin\varphi\right)^2 \left|E_{\pm}^{(l)}\right|^2, \qquad (37)$$

where φ is the azimuthal angle in the referent frame $x0y'$. We assume that the ordinary and extraordinary beams are separated in the asymptotic case and take into account only the field of the ordinary beam both in RHP and LHP beam components. The expression (37) shows that the mean square width $W_{\pm} = \sqrt{W_{\pm}^2}$ is a periodical function of the angle φ with a period 2π. It oscillates around the value: $\overline{W_{\pm}} = \frac{1}{\pi}\int_0^{\pi}\sqrt{W_{\pm}^2}\,d\varphi$. The deformation *D* relative to the asymptotic transverse shift Δx_T can be defined as $D(z, \alpha_o, l) = \left(W_{\max} - \overline{W}\right)/\Delta x_T$. The curve $D(z)$ shown in Fig. 14 illustrates deformation of the cross-section of the U - and $F-$beam components along the crystal length z. The U -beam deformation changes very slowly along the crystal in the LHP $U_{-}^{(3)}$ component and its magnitude is only $D = 0.02$ at the crystal length $z = 0.4\,m$ .The RHP component $U_{+}^{(3)}$ does not experience any deformation. Absolutely other situation is observed in the circularly polarized components $F_{+}^{(3)}$ and $F_{-}^{(3)}$ of the linearly polarized *F*-beams. The cross-sections of the linearly polarized beams are distorted even for the on-axis beams $\alpha_o = 0$ [42] for the zero transverse shift. When tilting the beam this effect is enhanced. However, the contribution of the transverse shift Δx_T to the deformation process, on our opinion, is negligible and such a deformation is inherent in all linearly polarized beams in the crystal [42].

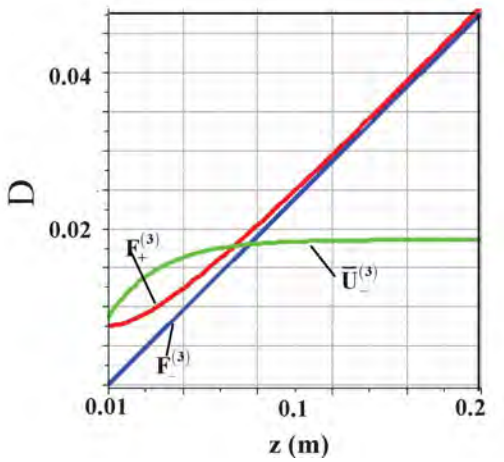

Fig. 14. Deformation D of the $U_-^{(3)}$, $F_+^{(-3)}$ and $F_-^{(-3)}$ beam components as a functions of the crystal length z: $\alpha_o = 10^o$, $w_0 = 50\,\mu m$.

CONCLUSIONS

We have discussed the destruction and recovery of high order paraxial vortex-beams in the unbounded medium of a uniaxial crystal when the beam propagates at a small angle to the crystal optical axis. We paid a special attention to the transverse shift of the beam induced by the homogeneous anisotropic medium. We have brought to light that three optical processes underline the transverse shift of the crystal traveling beam: dislocation reactions in the circularly polarized components, the beam depolarization and the spin-orbit coupling. It has been shown that an inclination of the beam relative to the crystal optical axis is tightly connected with a global reconstruction of the vortex structure. For example, a RHP singular beam bearing an optical vortex with a topological charge equal to *-l* at the crystal input stimulates appearance of the LHP singular beam with a topological charge *–l+2* when propagating along the crystal optical axis. When tilting the beam the LHP component of the beam loses two positively charged optical vortices while the RHP component keeps its former vortex composition. At the first glance it seems that both circularly polarized components carries over now identical optical vortices. However, we have shown that a fine structure of the beam core in the RHP and LHP components is different. All optical vortices gather together at the axis of the RHP component forming the *l*-charged optical vortex. At the same time, only *l-1* vortices gather together at the axis of the LHP component while one singly charged vortex is shifted along the direction perpendicular to the inclination plane of the beam. Besides, the beam is depolarized. These processes break the inner matching of the SAM and the OAM bound with the vortex topological charge. Such mismatching is removed by the spin-orbit coupling owing to the transverse shift of the LPH beam component. The transverse shift does not depend on a sign and magnitude of the vortex topological charge l in contrast to that in the Fedorov-Imbert effect [39]. However, the shift changes its direction to the opposite one

when switching the handedness of the initial circular polarization and changing a sign of the inclination angle α_o. In the initially linearly polarized beam, both circularly polarized components experience the transverse shift in opposite directions. This effect can be treated as *the beam quadrefringence* [18] in a uniaxial, homogeneous anisotropic medium. The first two beams is a result of the splitting of the total tilted beam into the linearly polarized ordinary and extraordinary ones. The appearance of the second two beams originates from the splitting of the linearly polarized beams into the circularly polarized components caused by the transverse shift. But such a transverse shift is a very small (about a half of the wavelength) and the effect is experimentally perceived as an ordinary beam birefringence. We have also analyzed the deformation of the beam cross-section caused by the transverse shift and revealed that deviations of the mean square width of the beam cross-section are vanishingly small.

ACKNOWLEDGMENTS

We are indebted to K. Yu. Bliokh for his valuable comments. We also thank E. Abramochkin for the useful discussion on the theoretical aspects of the work and B. Sokolenko for his help in the experiment.

References

1. Born M. Principles of Optics / M. Born, E. Wolf. – New York: Pergamon, 1975
2. Fleck J.A. Beam propagation in uniaxial anisotropic media / J.A. Fleck, M.D. Feit. // J. Opt. Soc. Am. – 1983. – V. 73. – P. 920-928.
3. Seshadri S.R. Basic elliptical Gaussian wave and beam in a uniaxial crystal / S.R. Seshadri // J. Opt. Soc. Am. A. – 2003. – V. 20. – P. 1818-1826.
4. Berry M.V. Conical diffraction: Hamilton's diabolical points at the heart of crystal optics / M.V. Berry, M.R. Jeffray // Progress in Optics. – 2007. – V. 50. – P. 11-50.
5. Volyar A.V. Generation of singular beams in uniaxial crystals / A. Volyar, T. Fadeyeva // Optics and Spectroscopy. – 2003. – V. 94. – P. 264-274.
6. Ciattoni A. Circular polarized beams and vortex generation in uniaxial media / A. Ciattoni, G. Cincotti, C. Palma // J. Opt. Soc. Am. A. – 2003. – V. 20. – P. 163-171.
7. Egorov Yu. The fine structure of singular beams in crystals: colours and polarization / Yu. Egorov, T. Fadeyeva, A. Volyar // J. Opt: Pure and Appl. Opt. – 2004. – V. 6. – P. S217-S228.
8. Volyar A. Laguerre-Gaussian beams with complex and real arguments in uniaxial crystals / A. Volyar, T. Fadeyeva // Optics and Spectroscopy. – 2006. – V. 101. – P. 297-304.
9. Soskin M. Singular optics / M. Soskin, M. Vasnetsov // Progress in Optics. – 2001. – V. 42. – P. 219.
10. Soskin M. Topological charge and angular momentum of light beams carring optical vortices / M. Soskin, V. Gorshkov, M. Vasnetsov, J. Malos, N. Heckenberg // Phys. Rev. A. – 1997. – V. 56. – P. 4064-4075.
11. O'Holleran K. Polarization Singularities in 2D and 3D Speckle Fields / K. O'Holleran, M.R. Dennis, F. Flossmann, and M.J. Padgett // Phys. Rev. Lett. – 2008. – V. 100 – P. 053902-1-4.
12. Nye J.F. *Natural Focusing and Fine Structure of Light: Caustics and Wave Dislocations* / J.F. Nye // New-York:CRC Press, 1999.
13. Dennis M.R. Polarization singularities in paraxial vector fields: morphology and statistics / M.R. Dennis // Optics Communications. – 2002. – V. 213. – P. 201.
14. Flossmann F. Fractality of Light's Darkness / F. Flossmann, K. O'Holleran, M. Dennis, M. Padgett // Phys. Rev. Lett. – 2008. – V. 100. – P. 203902-1-4.

15. Allen L. Optical Angular Momentum / L. Allen, S.M. Barnet, M.J. Padgett // Bristol:IOP Publishing, 2003. – 300 p.
16. Ciattoni A. Angular momentum dynamics of a paraxial beam in a uniaxial crystal / A. Ciattoni, G. Cincotti, C. Palma // Phys. Rev. E. – 2003. – V. 67. – P. 036618-1-10.
17. Brasselet E. Dynamics of optical spin-orbit coupling in uniaxial crystals / E. Brasselet, Ya. Izdebskaya. V. Shvedov, A. Desyatnikov, W. Krolikowsky and Yu. Kivshar // Optics Letters. – 2009. – V. 34. – P. 1021-1023.
18. Fadeyeva T. Quadrefringence of optical vortices in a uniaxial crystal / T. Fadeyeva, A. Rubass, Yu. Egorov, A. Volyar, G. Swartzlander // J. Opt. Soc. Am. – 2008. – V. 25. – P. 1643-1641.
19. Flossman F. Polarization singularities from unfolding an optical vortex through a birefringent crystal / F. Flossman, U.T. Schwarz, M. Maier, M.R. Dennis // Phys. Rev. Lett. – 2005. – V. 95. – P. 25390-1-4.
20. Chin S.Y. Gaussian beam in anisotropic media / S.Y. Chin, L.B. Felson // Applied Physics. – 1974. – V. 5. –P. 225-239.
21. Palma C. Decentered Gaussian beams, rays bundles, and Bessel-Gaussian beams / C. Palma // Appl. Opt. – 1997. – V. 36. – P. 1116-1120.
22. Zauderer E. Complex argument Hermite-Gaussian and Laguerre-Gaussian beams / E. Zauderer // J. Opt. Soc. Am. – 1986. – V. 3. – P. 465-469.
23. Flossmann F. Stokes parameters in the unfolding of an optical vortex through a birefringent crystal / F. Flossmann, U.T. Schwarz, M. Maier, M.R. Dennis // Optics Express. – 2006. – V. 14. – P. 11402-11411.
24. Fadeyeva T. Indistinguishability limit for off-axis vortex beams in uniaxial crystals / T. Fadeyeva, Yu. Egorov, A. Rubass, G.A. Swartzlander Jr, A. Volyar // Optics Letters. – 2007. – V. 32. – P. 3116-3118.
25. Freund I. Critical point explosions in two-dimensional wave fields / I. Freund // Optics Communications. – 1999. – V. 159. – P. 99-117.
26. Bath R. Mechanical detection and measurement of the angular momentum of light / R. Bath // Physical Review. – 1936. – V. 50. – P. 115-125.
27. Fedorov F.I. On the theory of a total reflection / F.I. Fedorov // Dokl. Akad. Nauk SSSR. – 1955. – V. 105. – P. 465-467.
28. Imbert C. Calculation and experimental proof of the transverse shift induced by total internal reflection of a circularly polarized light / C. Imbert // Phys. Rev. – 1972. – V. D5. – P. 787-796.
29. Bliokh K.Yu. Polarization, transverse shifts and angular momentum conservation laws in partial reflection and refraction of an electromagnetic wave packet / K.Yu. Bliokh, Yu.P. Bliokh // Physical Review E. – 2007. – V. 75. – P. 066609-1-10.
30. Aiello A. Role of propagation in Goos-Hanchen and Inbert-Fedorov shifts / A. Aiello, J.P. Woerdman // Optics Letters. – 2008. – V. 33. – P. 1437-1439.
31. Nasalski W. Displacement of the intensity peak in narrow beams reflected at a dielectric interface / W. Nasalski, T. Tamir, L. Lin // J. Opt. Soc. Am. A. – 1988. – V. 5. – P. 132-140.
32. Nasalski W. Longitudinal and transverse effects of nonspecular reflection / W. Nasalski // J. Opt. Soc. Am. A. – 1996. – V. 13. – P. 172-181.
33. Bliokh K.Yu. Conservation of angular momentum, transverse shift and spin Hall effect in reflection and refraction of an electromagnetic wave packet / K.Yu. Bliokh, Yu.P. Bliokh // Phys. Rev. Lett. – 2006. – V. 96. – P. 073903-1-4.
34. Hosten O. Observation of the spin Hall effect in light via weak measurements / O. Hosten, P. Kwist // Science. – 2008. – V. 319. – P. 787-790.
35. Onoda M. Hall effect in light / M. Onoda, S. Murakami, N. Nagaosa // Phys. Rev. Lett. – 2004. – V. 93. – P. 083901-1-4.
36. Liberman V.S. Optical Magnus effect / V.S. Liberman, B.Ya. Zel'dovich // Physical Review A. – 1992. – V. 46. – P. 5199.
37. Volyar A. Polarization splitting of the plane propagation of a local wave in a step-index multimode fiber / A. Volyar, A. Gnatovskii, S. Lapaeyeva, V. Myagkov // Ukraine Physical Journal. – 1992. – V. 37. – P. 1468-1471.
38. Bliokh K.Yu. Geometrical optics of beams with vortices and orbital angular momentum Hall effect / K.Yu. Bliokh // Physical Review Letters. – 2006. – V. 97. – P. 043901.

39. Fedoseyev V.G. Spin-independent transverse shift of the center of gravity of a reflected and of a refracted light beams / V.G. Fedoseyev // Optics Communications. – 2001. – V. 191. – P. 9-18.
40. Okuda H. Huge transverse deformation in nonspecular reflection of a light beam possessing orbital angular momentum near critical incidence / H. Okuda, H. Sasada // Optics Express. – 2006. – V. 14. – P. 8393-8402.
41. Ciatoni A. Anisotropic beam spreading in uniaxial crystals / A. Ciatoni, C. Palma // Optics Communications. – 2004. – V. 231. – P. 79-92.
42. Cincotti G. Laguerre-Gaussian and Bessel-Gaussian beams in uniaxial crystals / G. Cincotti, A. Ciatoni, C. Palma // J. Opt. Soc. Am. A. – 2002. – V. 19. – P. 1680-1688.

Фадеєва Т.А. Чотиризаломлення вихрових пучків у дволучезаломлюючих кристалах / Т.А. Фадеєва, О.Ф. Рибась, О.В. Воляр // Вчені записки Таврійського національного університету ім. В.І. Вернадського. Серія: Фізико-математичні науки. – 2010. – Т. 23(62), № 1. Ч. І. – С. 30-56.
Ми знайшли асиметричне розщеплення циркулярно поляризованих вихрових пучків вищого порядку в одновісьовому кристалі. Вихровий пучок з топологічним зарядом *L* розщеплюється на пучок з зарядом вихору *L-1*, що росповсюджується вздовж напрямку розповсюдження первісного пучку, та один оптичний вихор, зміщений у напрямку перпендикулярному площині нахилу пучку. Причиною такого зміщення вихору є боковий зсув парціального пучка. Ми розглядаємо ефект бокового зсуву як з точки зору закону збереження потоку кутового моменту, так й на базі рішення параксіального хвильового рівняння. Ми показали, що поперечний зсув пучка, після проходження кристала не залежить ні від величини, ні від знаку топологічного заряду оптичного вихору, та визначаються тільки первісною циркулярною поляризацією й кутом нахилу пучку.
Ключові слова: одновісьовий кристал, лазерне випромінювання, топологічний заряд, оптичний вихор, стан поляризації, поляризаційна сингулярність.

Фадеева Т.А. Четырепреломление вихревых пучков в двулучепреломляющих кристаллах / Т.А. Фадеева, А.Ф. Рыбась, А.В. Воляр // Ученые записки Таврического национального университета им. В.И. Вернадского. Серия: Физико-математические науки. – 2010. – Т. 23(62), № 1. Ч. І. – С. 30-56.
Мы нашли ассиметричное расщепление циркулярно поляризованных пучков высших порядков в одноосном кристалле. Вихревой пучок с топологическим зарядом *L* расщепляется на пучок с зарядом *L-1*, который распространяется вдоль направления распространения первоначального пучка и одиночный вихрь, смещенный в направлении перпендикулярном плоскости наклона пучка. Причиной такого смещения вихря есть боковое смещение парциального пучка. Мы рассматриваем эффект бокового смещения как с точки зрения закона сохранения потока углового момента, так и на основании решения параксиального волнового уравнения. Мы показали, что боковое смещение пучка, после прохождения кристалла не зависит ни от величины ни от знака топологического заряда оптического вихря, и обусловлен только первоначальной циркуляцией и углом наклона пучка.
Ключевые слова: одноосный кристалл, лазерное излучение, топологический заряд, оптический вихрь, состояние поляризации, поляризационная сингулярность.

Поступила в редакцию 16.12.2009 г.